Integration of Well Logging Analysis with Petrophysical Laboratory Measurements for Nukhul Formation at Lagia-8 Well, Sinai, Egypt

A. Z. NOAH[1] and T. F. Shazly[2]

[1]Faculty of Science and Engineering, The American University in Cairo, Egypt
[2]Egyptian Petroleum Research Institute, Cairo, Egypt

ABSTRACT

The objective of this paper is to analyze the petrophysical properties of the reservoir rock obtained by core analysis and well logs in order to spot some light on hydrocarbon potentiality for Nukhul Formation at the study well. Two core plugs (sample 1 and 2) have been obtained from Lagia-8 well in Lagia Field at depths 1296 and 1297 ft. respectively. Special core analysis has been performed on both core samples. Well logging data on Lagia-8 well has also been obtained and interpreted using Techlog® software.

Nukhul Formation contains biodegraded heavy oil at Lagia-8 well, and consists of five sandstone lobes that are interbedded with mudstones. The sandstones are typically fine to medium grained and well cemented with calcareous cement.

It has been found that, core analysis gives more accurate indication of well parameters as it involves real measurements of actual samples from the well. However, several parameters are not considered in core analysis such as reservoir temperature and pressure, invasion effects, and gas effects. Core analysis was conducted to measure porosity, grain density, permeability, water and hydrocarbon saturations and capillary pressure. Also well logging analysis using a set of well logging data was interpreted to measure the reservoir characteristics such as: porosity, volume of shale and both water and hydrocarbon saturation.

Nukhul Formation at the study well attains about 221 m. in thickness. From petrophysical analysis, it was found that, the average porosity of the reservoir was 0.27. The pores are filled with more than 27% of hydrocarbons. The measured core permeability was about 166.8 mD.

{**Citation:** A. Z. Noah, T. F. Shazly. Integration of well logging analysis with petrophysical laboratory measurements for nukhul formation at Lagia-8 Well, Sinai, Egypt. American Journal of Research Communication, 2014, 2(2): 139-146} www.usa-journals.com, ISSN: 2325-4076.

INTRODUCTION

The Lagia Field, (Fig. 1) is located onshore in the north western of Sinai, 26 km south of the Asl Field and is a part of the Central Sinai Concession. During the period 1949 – 2000

four wells (Lagia 3, Lagia 5, Lagia 6 and Lagia7) were drilled in Lagia Field. It is estimated that the Lagia Field might contain up to 89 MM barrels of 16-19 degrees API oil in place.

Figure 1. Location map for Lagia Field, Sinai, Egypt.

Nukhul Formation contains biodegraded heavy oil at Lagia Field, and consists of five sandstone lobes that are interbedded with mudstones. All lobes deeper than the first lobe have been truncated up dip or faulted out and are not present. The sandstones are typically fine to medium grained and well cemented with calcareous cement. Table (1) exhibits some details for the formations in the study well.

Table 1. Formation details for the study area

Formation Name	Formation Top (ft)	Formation TVD (ft)	Formation Thickness (ft)	Lithology Types
RUDIES	SURFACE	SURFACE	----	Shale, Limestone and Gypsum
NUKHUL	1133	-1000	221	Sandstone, Limestone and shale
EOCENE	1354	-1221	106	Limestone.

I. ROUTINE CORE ANALYSIS OF LAGIA-8 CORE SAMPLES

Special core analysis was performed on two core plugs (sample 1 and sample 2) that taken from Lagia-8 well in Lagia Field at depth 1296 and 1297 ft. respectively. The experiments were conducted in The American University in Cairo Core Lab.

I.1. Porosity Measurement

Measurement of porosity was carried out by application of Gas expansion using Helium Porosimeter. This method relies on the ideal gas law, or rather Boyle's law. The rock is sealed in a container of known volume V_1 at atmospheric pressure P_1 (Fig. 2). This container is attached by a valve to another container of known volume, V_2, containing gas at a known pressure, P_2.

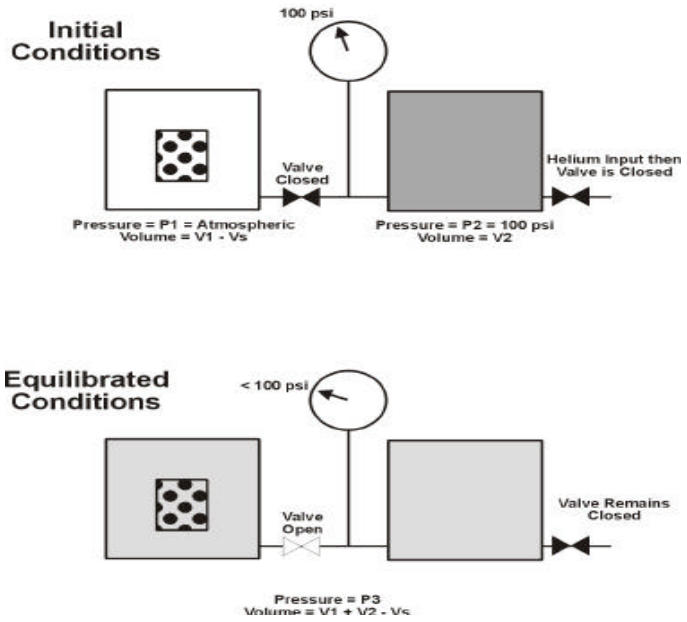

Figure 2. Helium porosimeter.

When the valve that connects the two volumes is opened slowly so that the system remains isothermal, the gas pressure in the two volumes equalizes to P_3. The value of the equilibrium pressure can be used to calculate the volume of grains in the rock (Vs) as shown in equation 1 and 2. Boyle's Law states that the pressure times the volume for a system is constant. Thus we can write the PV for the system before the valve is opened, left hand side of Eq. (1), and set it equal to the PV for the equilibrated system, right hand side of Eq. (2):

$$P_1(V_1 - V_s) + P_2V_2 = P_3(V_1 + V_2 - V_s) \quad (1)$$

$$V_s = (P_1V_1 + P_2V_2 - P_3(V_1 - V_2)) / (P_1 - P_2) \quad (2)$$

In practice P_1, P_2 and P_3 are measured, with V_1 and V_2 are known in advance by calibrating the system with metal pellets of known volume. The bulk volume of the rock is determined before the experiment by using either vernier calipers and assuming that the sample is perfectly cylindrical, or after the experiment and subsequent saturation by Archimedes Method (discussed later), or by fluid displacement using the saturated sample. The bulk volume and grain volume can then be used to calculate the connected porosity of the rock. Any gas can be used, but the commonest is helium. The small size of the helium

molecule means that it can penetrate even the smallest pores. Consequently this method gives higher porosities than either the imbibition or mercury injection methods. The method itself is very accurate, insensitive to mineralogy, and leaves the sample available for further petrophysical tests. It is also a rapid technique and can be used on irregularly shaped samples. Inaccuracies can arise with samples with very low permeability. Low permeability samples can require long equilibration times in the helium porosimeter to allow diffusion of helium into the narrow pore structures. Failure to allow adequate time will result in excessively high grain volumes and low porosities. Table (2) shows the porosimeter results.

Table 2. Porosimeter results

Sample NO.	**1**	**2**
Sample diameter (mm)	25.33	25.23
Sample Length (mm)	61.91	31.06
Bulk volume (cc)	31.20	15.53
Weight (g)	61.14	30.33
Grain Volume (cc)	22.41	11.19
Pore volume (cc)	8.79	4.34
Grain density (g/cc)	2.73	2.71
Core Porosity	0.28	0.28
P_{ref} (Psi)	99.99	100.05
P_{exp} (psi)	68.01	60.29
P ratio	1.47	1.66

1.2. Grain Volume Measurement

The grain volume of core samples is sometimes calculated from sample weight and knowledge of average density. Boyle's law is often employed with helium as the gas to determine grain volume. The technique is fairly rapid, and is valid on clean and dry samples. The measurement of the grain volume of a core sample may also be based on the loss in weight of a saturated sample plunged in a liquid. Grain volume may be measured by crushing a dry and clean core sample. The volume of crushed sample is then determined by either pycnometer or immersing in a suitable liquid.

1.3. Permeability Measurement

When the core plugs are completely dried from all fluids and their dimensions are measured, the core plugs are tested on the gas permeameter as shown in Fig. (3). The core sample is placed inside the sample cell, and the computer application "Invoke appli Lab" is started. The equipment is turned on and left for 30 minutes before using it. The following operations are followed:

1. The nitrogen gas cylinder is opened and the pressure is adjusted using the cylinder's pressure regulators; the upstream pore pressure is set to 4.9 psi and confining pressure to 400 psi.
2. Using the software, the following data is entered. Note that the actual dimensions and names of the core sample are in Fig. (4).
3. After the data is entered, the confining pressure valve is rotated from "vent" to "pressure" position.
4. The flow rate is adjusted using the flow rate knob.
5. The software will record the downstream pressure when the upstream pressure stabilizes.
6. After pressure stabilizes, the flow rate is increased to another value until the pressure stabilizes and recorded by the software. This step is repeated several times for each core sample (sample 1 was repeated 6 times and sample 2 was repeated 9 times). The results are shown in Table (3).

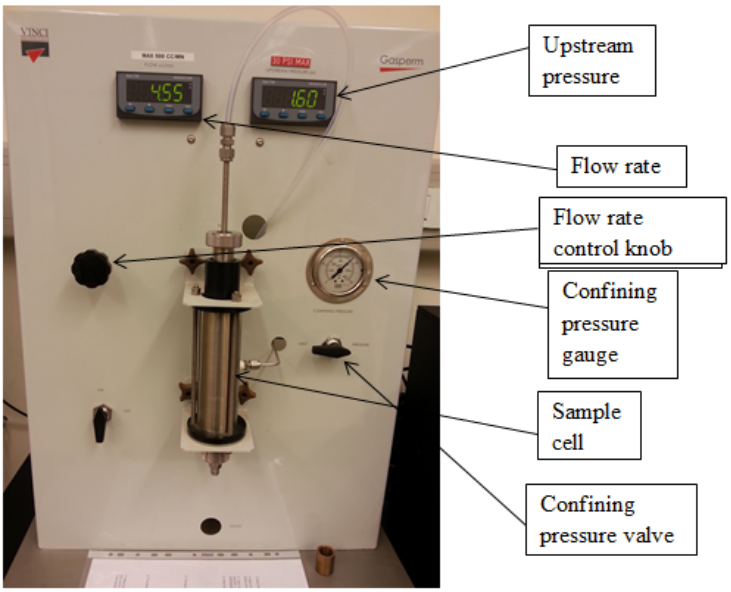

Figure 3. Gas permeameter.

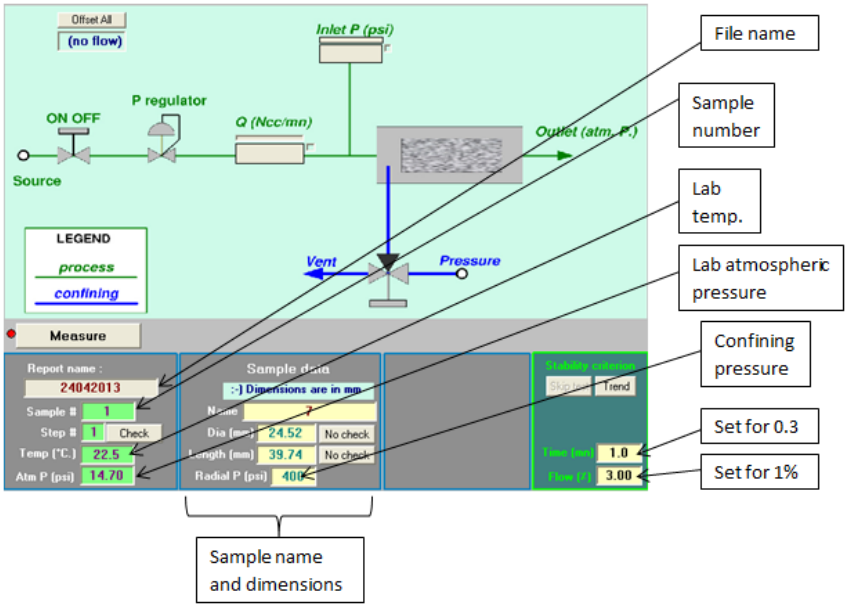

Figure 4. Invoke appli Lab layout.

Table 3. Results spreadsheet

	A	B	C	D	E	H	J	K	M	N	Q	U	V
10	Sample N°	Sample Name	Dia (mm)	Length (mm)	Atm. Press. (psi)	Confining Pressure Radial (psig)	Date Time of test	PT01 (psig)	Temp. (°C)	FQT01 (Ncc/min)	Ka (mD)	Darcy conditions granted	Measured at stabilisation
11		1	25.33	61.91	14.70	400	21-4-13 2:57 PM	1.57	22.5	4.540	15.728	OK	OK
12		1	25.33	61.91	14.70	400	21-4-13 3:00 PM	2.16	22.5	6.250	15.443	OK	OK
13	1	1	25.33	61.91	14.70	400	21-4-13 3:04 PM	3.41	22.5	9.830	14.800	OK	OK
14		1	25.33	61.91	14.70	400	21-4-13 3:06 PM	5.16	22.5	14.930	14.102	OK	OK
15		1	25.33	61.91	14.70	400	21-4-13 3:08 PM	7.13	22.5	20.590	13.316	OK	OK
16		1	25.33	61.91	14.70	400	21-4-13 3:16 PM	7.45	22.5	21.530	13.210	OK	OK
17													NO
18	2												OK
19													NO
20													NO
21		2	25.23	31.06	14.70	400	21-4-13 3:23 PM	0.47	22.5	4.350	26.393	OK	OK
22		2	25.23	31.06	14.70	400	21-4-13 3:26 PM	0.73	22.5	6.830	26.450	OK	OK
23	3	2	25.23	31.06	14.70	400	21-4-13 3:37 PM	1.87	22.5	17.090	24.895	OK	OK
24		2	25.23	31.06	14.70	400	21-4-13 3:40 PM	2.42	22.5	22.100	24.446	OK	OK
25		2	25.23	31.06	14.70	400	21-4-13 3:43 PM	2.81	22.5	25.680	24.167	OK	OK
26		2	25.23	31.06	14.70	400	21-4-13 3:45 PM	3.16	22.5	28.880	23.909	OK	OK
27		2	25.23	31.06	14.70	400	21-4-13 3:47 PM	3.84	22.5	35.120	23.437	OK	OK
28	4	2	25.23	31.06	14.70	400	21-4-13 3:51 PM	3.85	22.5	35.260	23.462	OK	OK
29		2	25.23	31.06	14.70	400	21-4-13 3:53 PM	3.95	22.5	36.240	23.433	OK	OK

The description of the core samples are as follow:
For core sample 1:
Length: 61.91 mm = 6.91 cm, Diameter: 25.33 mm = 2.53 cm, Cross Section Area = $\frac{\pi}{4}d^2 = \frac{\pi}{4}(2.53)^2 = 5.03\ cm^2$.

Table (4) shows pressures and flow rates of sample 1. P_1 is the upstream pressure, P_2 is the downstream pressure, and Q is the upstream flow rate. Downstream flow rate is zero therefore it is neglected. K_g is calculated using Darcy's law.

Table 4. Gas permeability results for sample 1.

P_1 (psig)	P_1 (atm)	P_2 (atm)	P_m (atm)	$1/P_m$ (atm^{-1})	Q (cm^3/min)	Q (cm^3/sec)	K_g (mD)
1.57	1.107	1	1.054	0.949	4.54	0.076	15.728
2.16	1.147	1	1.074	0.932	6.25	0.104	15.443
3.41	1.232	1	1.116	0.896	9.83	0.164	14.800
5.16	1.351	1	1.176	0.851	14.93	0.249	14.102
7.13	1.484	1	1.242	0.805	20.59	0.343	13.316
7.45	1.506	1	1.253	0.798	21.53	0.359	13.210

The equivalent liquid permeability can be determined by plugging the average value of K_g and $1/P_m$ into the equation (Holditch, 1998):

$K_g = K_L + [6.9 (K_L)^{-0.36}] (K_L) (1/P_m)$ (3)

$K_{g\ avg.} = (15.728+15.443+14.8+14.102+13.316+13.21) / 6 = 14.433$ mD (4)

$(1/P_m)_{avg} = (0.949+0.932+0.896+0.851+0.805+0.798) / 6 = 0.872\ atm^{-1}$ (5)

After inserting the values the equation becomes:

$14.433 = K_L + [6.9 (K_L)^{-0.36}] (K_L) (0.872)$ (6)

By Solving for K_L, the equivalent liquid permeability or absolute permeability of sample 1 will be 2.80 mD.

For core sample 2:

Length: 31.06 mm = 3.106 cm, Diameter: 25.23 mm = 2.523 cm, Cross Section Area = $\frac{\pi}{4}d^2 = \frac{\pi}{4}(2.523)^2 = 4.999\ cm^2$.

Table (5) shows pressures and flow rates of sample 2.

Table 5. Gas permeability results for sample 2

P_1 (psig)	P_1 (atm)	P_2 (atm)	P_m (atm)	$1/P_m$ (atm^{-1})	Q (cm^3/min)	Q (cm^3/sec)	K_g (mD)
0.47	1.032	1	1.016	0.984	4.35	0.073	26.393
0.73	1.050	1	1.025	0.976	6.83	0.114	26.450
1.87	1.127	1	1.064	0.940	17.09	0.285	24.895
2.42	1.164	1	1.082	0.924	22.1	0.368	24.446
2.81	1.191	1	1.095	0.913	25.68	0.428	24.167
3.16	1.215	1	1.107	0.903	28.88	0.481	23.909
3.84	1.261	1	1.130	0.885	35.12	0.585	23.437
3.85	1.262	1	1.131	0.884	35.26	0.588	23.462
3.95	1.268	1	1.134	0.882	36.24	0.604	23.433

The equivalent liquid permeability can be estimated by plugging the average value of K_g and $1/P_m$ into the equation:

$K_g = K_L + [6.9 (K_L)^{-0.36}] (K_L) (1/P_m)$ (7)

$K_{gavg.}=(26.39+26.45+24.895+24.446+24.167+23.909+23.44+23.46+23.43)/9=24.51$mD (8)

$(1/P_m)_{avg} = (0.98+0.976+0.94+0.924+0.913+0.90+0.885+0.884+0.882) / 9 = 0.921\ atm^{-1}$ (9)

By substitution, the equation becomes:

$24.51 = K_L + [6.9 (K_L)^{-0.36}] (K_L) (0.921)$ (10)

Solving for K_L, the equivalent liquid permeability or absolute permeability of sample 2 equal 5.53 mD.

II. SPECIAL CORE ANALYSIS OF LAGIA-8 CORE SAMPLES

II.1. Relative Permeability Measurement

Laboratory measurements are conducted either by displacing one phase with another (unsteady state tests) or simultaneous flow of two phases (steady state tests). The steady-state method for a two-fluid system basically involves injecting two phases at a certain volumetric ratio until stabilization of both the pressure drop across the core and the effluent volumetric ratios (Charles, 1981). The saturation of the fluids in the core is determined by weighting the core or performing a mass-balance calculation of each phase. The unsteady-state method is based on the interpretation of an immiscible displacement process. The core, either preserved or cleaned, is flooded with one of the displacing fluids. Typically it is water, which is the case for our experiment (Dandekar, 2006).

Unsteady state tests are less time consuming than steady state tests, but can suffer from uneven saturation distributions (end effects). Displacement rates can be modified to accommodate wettability characteristics and to model reservoir flow rates. Steady state tests can be set up to avoid end effects but are more time consuming, requiring time to reach equilibrium at each chosen oil/water flow ratio. The effective permeability measured over a range of fluid saturations enable relative permeability curves to be constructed (Bed and Nunes, 1984). The experimental apparatus for relative permeability is shown in Fig. (4), while the unsteady state water flood procedure is shown in Fig. (5).

The experiment is done in the direction of the increasing water saturation to simulate water injection or water flooding in the reservoir. The base permeability can be the absolute permeability or the effective oil permeability at the irreducible water saturation (S_{wi}). In our case, it is the effective oil permeability at S_{wi} (Engler, 2003). Therefore, oil flooding is required. It is usually performed at constant flow rate to reach irreducible water saturation and continuous until a steady pressure drop is obtained. The effective permeability is measured using direct application of Darcy's law, (Sandberg and Sippel, 1993). In the core plug used, water is the wetting-phase and relative permeability are measured by the displacement of oil by water. If water displaces oil, the curves are called imbibition curves. On the other hand, if oil displaces water, the curves are called drainage curves. Imbibition curves are important for water flood calculations, water influx, and oil displacing gas while drainage curves are important for solution gas drive, gravity drainage (gas displaces drained oil), and gas injection processes (Dandekar, 2006).

Figure 4. Relative permeability experimental apparatus.

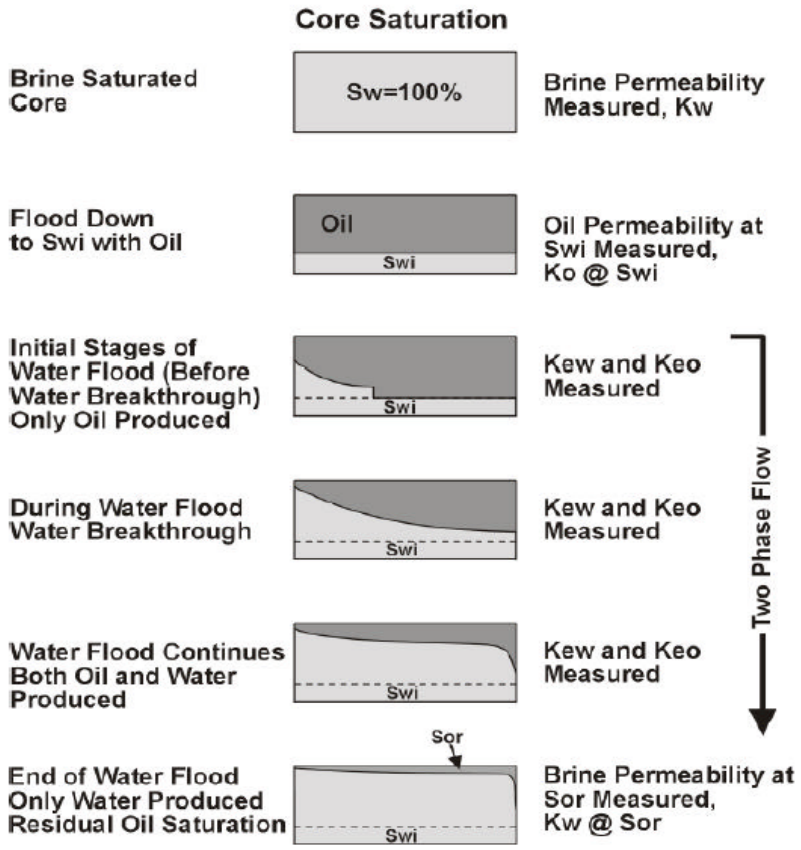

Figure 5. Unsteady state water flood procedure (Sandberg and Sippel, 1993).

The Dean-stark values can be used in reconfirming the initial fluid saturations in the core plug sample. After the core plug sample is cleaned using the Dean-stark, the core plug is saturated with formation water under a pressure of 2000 psi. When the core plug is fully saturated with water, the absolute permeability of the sample is determined using Darcy's law. Next, oil is injected in the core plug sample saturated with formation water until no more water is produced. Based on the produced total amount of water and the measured pore volume of the core plug, the amount of irreducible water inside the core plug can be calculated by subtracting the produced water from pore volume. However, the initial water saturation that was established in the reservoir due to the hydrocarbon migration process differs from that measured experimentally in the lab (Glover, 2001 and 2012).

When the core plug is initially 100% saturated with formation water at 2000 psi, the flow rate of water and the differential pressure are measured to calculate the absolute permeability. The base permeability will be taken as the effective permeability to oil at $S_{wi,}$ Table (6) includes Q, ΔP, and K for formation water flowing through the core plug.

Table 6. Water flood (100% saturated)

Q (cc/min)	ΔP (psi)	K_{eff} (mD)
0.5	0.95	210.67
1	2	200.13
2	4.2	190.60
3	6.6	181.94
4	9.2	174.03
5	11.6	172.53
6	14	171.54
7	16.4	170.84

By plotting ΔP versus Q the slope will be:
Slope = $\mu \cdot L / A \cdot K = 1.634/K$ (11)
Q is converted to cc/sec and Δ P is converted to atm, K = 1.634/slope where the slope is found to be 9.795 as shown in Fig. (6).

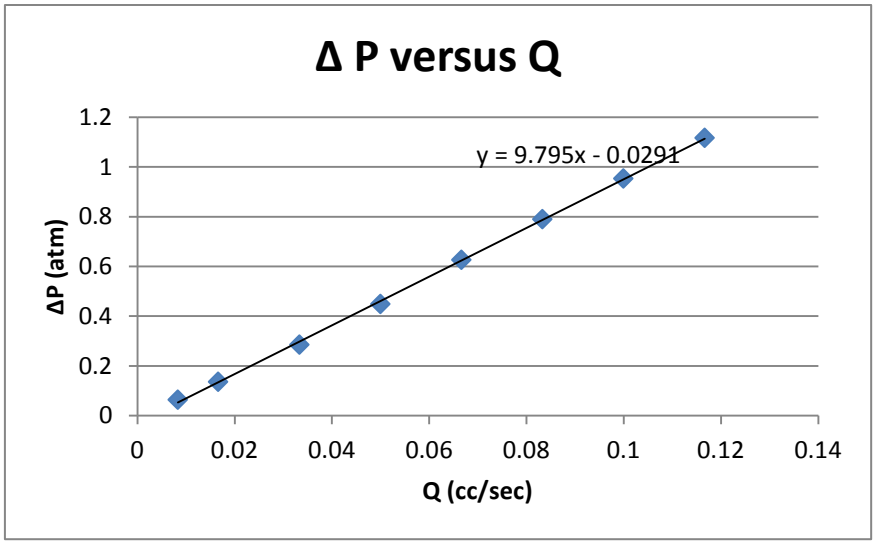

Figure 6. Presuure versus rate of flow for Lagia -8 well.

Absolute permeability can be determined at 100% saturation with formation water through the following equation:
$(K_{abs}) = [1.634/9.795] * 1000 = 166.82$ mD. (12)

II.2. Effective Permeability

After determining the absolute permeability, the estimation of the effective permeability to oil at irreducible water saturation (K_{eo} @ S_{wi}) was wanted. Oil is injected at a flow rate of oil of 6 cc/min. Oil flows throughout the core plug, displacing water until the last droplet or bubble of water is released (Dandekar 2006). At this point, we have reached the irreducible water saturation (S_{wi}). Thus, knowing the amount of water displaced and the initial pore volume occupied by water, we can measure the residual water saturation (S_{wi}). The effective

permeability to oil at S_{wi} is measured using Darcy's law based on the following parameters summarized in Table (7).

Table 7. Drainage data for lagia -8 well.

Drainage	
Flow rate (cc/min)	6
Final ΔP (psi)	135.3
Drainage DV (cc)	2.6
V_{water} burette (cc)	7.5
V_{wi} (cc)	2.44
S_{wi} (%)	33.24
K_{eo} (S_{wi})	2.65
K_{ro} (S_{wi})	1

Dead volume is the volume of fluid stored outside the core sample. For oil, the dead volume of water is 2.6 cc. The volume of displace water d is 7.5 cc as shown in Figs. (7 and 8)**,** but 2.6 cc is not inside the core plug (dead volume). Therefore, the actual volume of displaced water is 7.5 – 2.6 = 4.9 cc. The volume of remaining water inside the core plug is determined by subtracting the produced water volume from the pore volume, which is 7.34 – 4.9 = 2.44 cc (irreducible water volume). The irreducible water saturation is found by dividing the irreducible water volume by the total pore volume.

$$S_{wi} = \frac{\text{Irreducible water volume}}{\text{Total pore volume}} = \frac{2.44}{7.34} = 33.24\ \% \quad (13)$$

$$K_{eo} = \frac{Q \cdot \mu \cdot L}{A \cdot \Delta P} = \frac{(6/60)(2.9)(6.191)}{(5.04)(135.3 * 0.068)} = 0.03872\ D = 38.72\ mD \quad (14)$$

$$K_{ro} = \frac{Keo}{Kbase} = \frac{Keo}{Keo} = \frac{38.72}{38.72} = 1 \text{at } S_{wi} \quad (15)$$

Figures 7 and 8. Oil displacing water to measure Swi (left); total displaced water volume (right).

Water is then injected during the process of imbibition at a rate of 0.2 cc/min where water saturation increases until it reaches the residual oil saturation (S_{or}). We can determine the point of breakthrough in which the first droplet of water is produced. Also we can estimate

the recovery factor of the reservoir by measuring the total volume of oil collected from the initial oil volume inside the core plug. The maximum effective permeability of water at S_{or} can also be calculated. Imbibition data and information are summarized in Tables (8 and 9).

Table 8. Imbibition data of Lagai-8 well.

Imbibition					
Time (min)	**ΔP (psi)**	**V_{oil}(cc)**	**V_{oil} (cc) cumulative**	**V_{water} (cc)**	**V_{water} (cc) cumulative**
10:14.2	6.5	1.6	1.6	0.0	0.0
26:02.0	10.1	2.3	3.9	0.05	0.05
0:48:23	10.4	0.3	4.2	4.2	4.25
1:27:55	9.3	0.2	4.4	7.6	11.85
2:09:09	8.5	0.25	4.65	8.9	20.75
2:51:04	8	0.2	4.85	8.0	28.75
3:51:51	7.7	0	4.85	12.1	40.85

Table 9. Imbibition information of Lagai-8 well.

Imbibition Information	
Start Time	**11:05:00 AM**
End Time	**2:56:51 PM**
Flow rate (cc/min)	**0.2**
Final Δ P (psi)	**7.7**
Imbibition DV (cc)	**1.3**
Breakthrough	**11:31:02 AM**
V_{oil} burette (cc)	**4.85**
V_{or} (cc)	**1.35**
Sor (%)	**18.4**
K_{ew} (Sor)	**0.71**
K_{rw} (Sor)	**0.27**

The time of breakthrough was found to be 26:02.0, when the first droplet of water was produced. The total volume of collected oil was 4.85 cc. The dead volume of oil is 1.3 cc. Therefore, the actual oil volume released from the core plug was 4.85 – 1.3 = 3.55 cc. The residual oil volume is determined by subtracting the produced oil volume from the initial oil volume in place, which is 4.9 – 3.55 = 1.35 cc. Residual oil saturation can then be calculated by dividing the residual oil volume by total pore volume. The total volume of oil displaced by water is the summation of the oil volumes in the test tubes as shown in Fig. (9).

$$S_{or} = \frac{\text{Residual oil volume}}{\text{Total pore volume}} = \frac{1.35}{7.34} = 18.39\ \% \quad (16)$$

$$K_{ew} = \frac{Q \cdot \mu \cdot L}{A \cdot \Delta P} = \frac{(0.2/60)(1.33)(6.191)}{(5.04)(7.7*0.068)} = 0.01040\ D = 10.4\ mD \quad (17)$$

$$K_{rw} = \frac{Kew}{Kbase} = \frac{Kew}{Keo} = \frac{10.4}{38.72} = 0.2686 \text{at } S_{or} \quad (18)$$

$$\text{Recovery at breakthrough} = \frac{\text{Oil produced @ breakthrough}}{\text{Initial oil in place}} = \frac{3.9-1.3}{4.9} = 53.06\ \% \quad (19)$$

$$\text{Total Recovery} = \frac{\text{Oil produced}}{\text{Initial oil in place}} = \frac{3.55}{4.9} = 72.45\ \% \qquad (20)$$

Figure 9. Imbibition test results to measure Sor.

As the irreducible water saturation and the residual oil saturation were known, the current water and oil saturation at any particular time during water flooding can be calculated. The volume of oil being displaced by water is the same as the volume of water entering the core sample. Adding the irreducible water volume to it, the total water volume in the sample can be known and the water saturation (S_w) at time X can be calculated. Oil saturation (S_o) is 1 minus the water saturation. Since one phase is being displaced by another immiscible phase, we have an unsteady state flow. Darcy's law is used to calculate the effective permeability for oil and water. Since water is injected at a constant rate of 0.2 cc/min. material balance is done by adding the flow rates of oil and water released to ensure that there are almost no losses within the system. Table (10) shows the flow rates out of oil and water.

Table 10. Oil and water flow rates out

Oil flow rate out (cc/min)	Water flow rate out (cc/min)	Total flow rate (cc/min)
0.16	0	0.16
0.14375	0.06105	0.2048
0.0136	0.191	0.2046
0.0051	0.195	0.2001
0.0059	0.212	0.2179
0.00476	0.19	0.19476
0	0.202	0.202

The following equations are used to generate the relative permeability as shown in Table (11). The relative permeability curve is shown in Fig. (10).

$$S_w = (V_{ir} + V_{oil\ cum} - 1.3) / PV \qquad (21)$$

$$S_o = 1 - S_w \qquad (22)$$

$$K_{eo} = \frac{Qo \cdot \mu \cdot L}{A \cdot \Delta P} \text{ where } Q_o = \frac{Voil\ cum(t) - Voil\ cum(t-1)}{\Delta t} \qquad (23)$$

$$K_{ew} = \frac{Qw \cdot \mu \cdot L}{A \cdot \Delta P} \text{ where } Q_o = \frac{Vwater\ cum(t) - Vwater\ cum(t-1)}{\Delta t} \quad (24)$$

$$K_{ro} = \frac{Keo}{Kbase} = \frac{Keo}{Keo\ @\ Swi} \quad (25)$$

$$K_{rw} = \frac{Kew}{Kbase} = \frac{Kew}{Keo\ @\ Swi} \quad (26)$$

Table 11. Relative permeability results for Lagia-8 well

Time (min)	ΔP (psi)	V_{oil} (cc)	V_{oil} (cc) cumulative	V_{water} (cc)	V_{water} (cc) cumulative	Sw	So	Keo	Kro	Kew	Krw
0:00	135.3	0	0	0	0	0.332	0.668	38.719	1.000	0.000	0.000
0:10	13	1.6	1.6	0	0	0.373	0.627	21.009	0.543	0.000	0.000
0:26	10.1	2.3	3.9	0.05	0.05	0.687	0.313	10.299	0.266	2.420	0.063
0:48	10.4	0.3	4.2	4.2	4.25	0.728	0.272	7.288	0.188	6.478	0.167
1:27	9.3	0.2	4.4	7.6	11.85	0.755	0.245	4.699	0.121	8.396	0.217
2:09	8.5	0.25	4.65	8.9	20.75	0.789	0.211	3.698	0.096	9.987	0.258
2:51	8	0.2	4.85	8	28.75	0.816	0.184	3.094	0.080	10.233	0.264
3:51	7.7	0	4.85	12.1	40.85	0.816	0.184	2.372	0.061	10.505	0.271

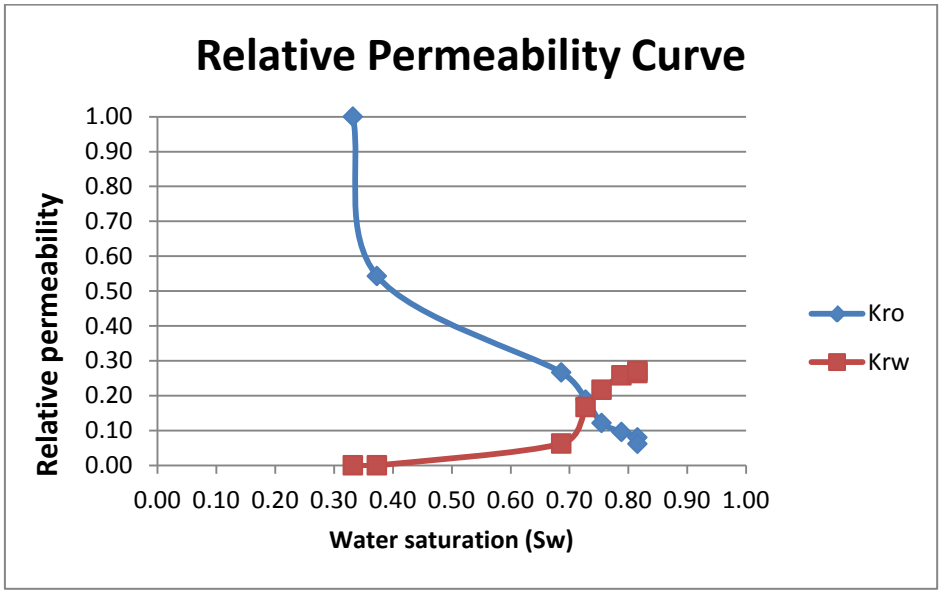

Figure 10. Relative permeability curve of Lagia -8 well.

II.3. Capillary Pressure Measurement

Capillary pressure is typically measured in the laboratory by using mercury injection, porous plate, or centrifugation techniques. The porous plate method, although time consuming, is considered the most direct and accurate method for capillary pressure measurements in the laboratory.

This technique is generally applied in the drainage mode to air-brine systems starting with test plugs which are initially brine saturated. The capillary pressure is applied across the test plug and a brine saturated porous plate. The high displacement pressure of the porous plate allows brine from the plug to pass through, but prevents flow of the displacing fluid (normally air). The apparatus is shown in Fig. (11). Plugs are removed at intervals and weighed until weight (and therefore fluid) equilibrium is attained. The applied pressure is then increased and the process repeated until a full curve of about six points is obtained (Ahmed, 2006).

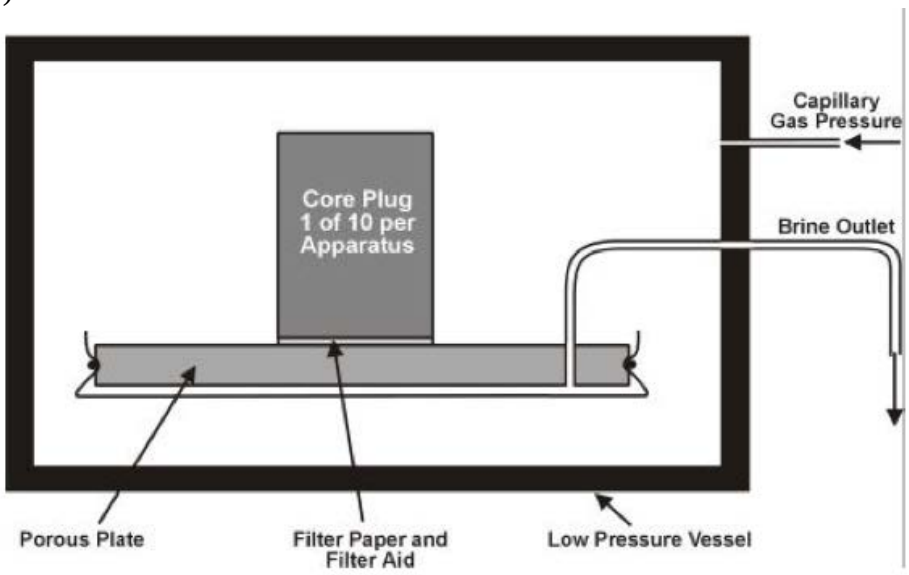

Figure 11. Porous plate measurement arrangement.

In this method care has to be taken to maintain good capillary contact between the test plug and the porous plate. This is assisted by using a paste of filter-aid and brine between the plate and a filter paper. The test plug is positioned on the paper and a lead weight placed on the plug to keep it solidly in place. There is also the danger that the water in the sample will be evaporated by the gas pressure. To avoid this, the input gas can be saturated with water by bubbling it through a reservoir of water prior to use, and keeping a beaker of water inside the porous plate pressure vessel (Amyx, 1960).

The resulting data is presented as (i) air-brine capillary pressure versus brine saturation, and then (ii) converted to oil-brine data, or (iii) as saturation versus height above oil-water contact.

II.3.1. Air-brine capillary pressure results

The following parameters represent the properties of the tested plug and the used brine.
$\Phi = 0.2795$, Length = 3.106 cm, Diameter = 2.523 cm, $\rho_{brine} = 1.08$ g/cm^3.
Table (12) exhibits the different results as shown:

Table 12. Air-brine capillary pressure data

Capillary pressure (psi)	Weight of plug after applying pressure (g)	Weight of brine lost (g)	Weight of brine remaining (g)	Volume of brine remaining (cm^3)	S_w
0	34.257	0.000	3.965	3.671	84.59%
1	33.890	0.367	3.598	3.331	76.76%
5	31.650	2.607	1.358	1.257	28.97%
10	31.508	2.886	1.079	0.999	23.01%
20	31.340	2.917	1.048	0.970	22.36%
30	32.310	2.925	1.040	0.963	22.18%
40	32.770	2.934	1.031	0.954	21.99%
50	32.180	2.938	1.027	0.951	21.91%

Fig. (12) represents a relationship between the capillary pressure and water saturation which is called air-brine capillary curve.

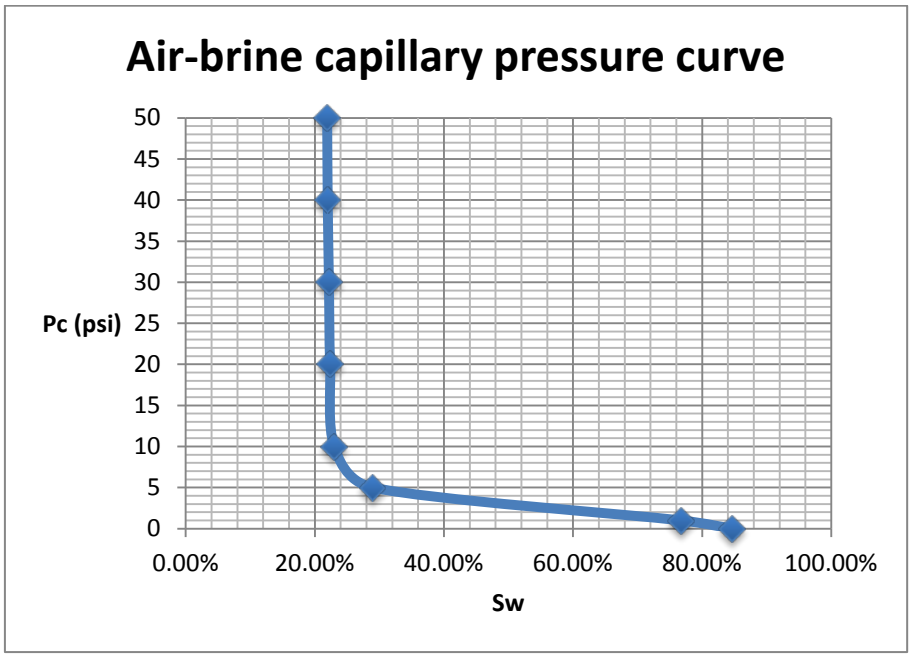

Figure 12. Capillary pressure versus water saturation for Lagia -8 well (sample 1).

Based on the above drainage curve (Fig. 12), the irreducible water saturation can be determined it is about 22%. The transition zone is the interval over which the saturation changes from its maximum value to its minimum irreducible saturation; it lies between capillary pressure values of 0 and 10 psi respectively. Therefore, we are interested only in comparing this part of the curve with the capillary pressure curve constructed using the saturation vs. height values obtained from the logs.

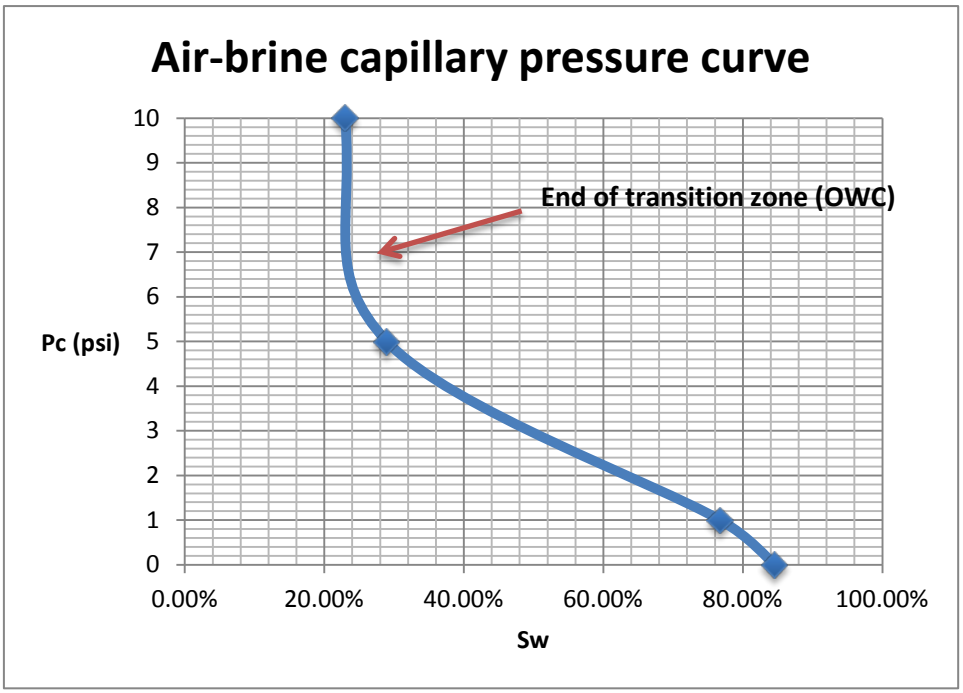

Figure 13. End of transition zone, oil/water contact (OWC) (sample 2).

In Fig. (13), based on the above magnified capillary pressure curve, we can determine the end of the transition zone, or in other words, the oil-water contact, which lies at a capillary pressure of 7 psi.

II.3.2. Air-brine to oil-brine conversion of capillary pressure results

In order to convert any capillary pressure values obtained in the lab to their equivalent reservoir capillary pressure data, we must be aware of the 4 different parameters that affect this conversion process. These parameters are:

i) Interfacial tension between the fluids used in the lab experiment.
ii) Contact angle between the fluids used in the lab experiment.
iii) Interfacial tension between the fluids present in the reservoir.
iv) Contact angle between the fluids present in the reservoir.

In our case, the two fluids used to calculate the capillary pressure data vs. saturation in the lab are reservoir brine and air. Therefore, we are interested in the values of both the air-water interfacial tension (σ_{wa}), and the air-water contact angle (θ_{wa}). On the other hand, the two fluids present in the reservoir are reservoir brine and oil. Therefore, we are interested in the values of both the oil-water interfacial tension (σ_{wo}), and the oil-water contact angle in the reservoir (θ_{wo}). The values used in the conversion from laboratory values of capillary pressure ($P_{c,lab}$) to reservoir values of capillary pressure ($P_{c,res.}$) are as follows:

σ_{wa} = 72 dyne/cm, θ_{wa} = 20° (an average value for water wet cores), σ_{wo} = 21 dyne/cm (based on the density of oil used), θ_{wo} = 30° (an average value and assuming that the reservoir becomes less water wet in the presence of oil, a phenomenon known as hysteresis). Using the above-mentioned values, a simple equation can be used to convert the capillary pressure lab values to reservoir values:

$$P_{c,res.} = \frac{\sigma_{wo}\cos\theta_{wo}}{\sigma_{wa}\cos\theta_{wa}} P_{c,lab} \qquad (27)$$

By substituting the values in the above equation:

$P_{c,res.} = 0.2688 P_{c,lab}$ (28)

Also, we have to convert the capillary pressure at which the transition zone ends (7 psi) to its equivalent reservoir capillary pressure. Therefore, the reservoir capillary pressure at which the transition zone ends is 1.8816 psi. This value is of extreme importance because it will be used to calculate the thickness of the transition zone and then will be compared with the value of the transition zone thickness obtained from the logs to validate our experimental work.

The oil-brine capillary pressure results are shown in Table (13). Figs (14 and 15) exhibit the oil-brine capillary pressure curve which is a relation between capillary pressure and water saturation.

Table 13. Oil-brine capillary pressure results.

S_w	$P_{c,lab}$(psi)	$P_{c,res.}$ (psi)
84.59%	0	0.00
76.76%	1	0.27
28.97%	5	1.34
23.01%	10	2.69
22.36%	20	5.38
22.18%	30	8.06
21.99%	40	10.75
21.91%	50	13.44

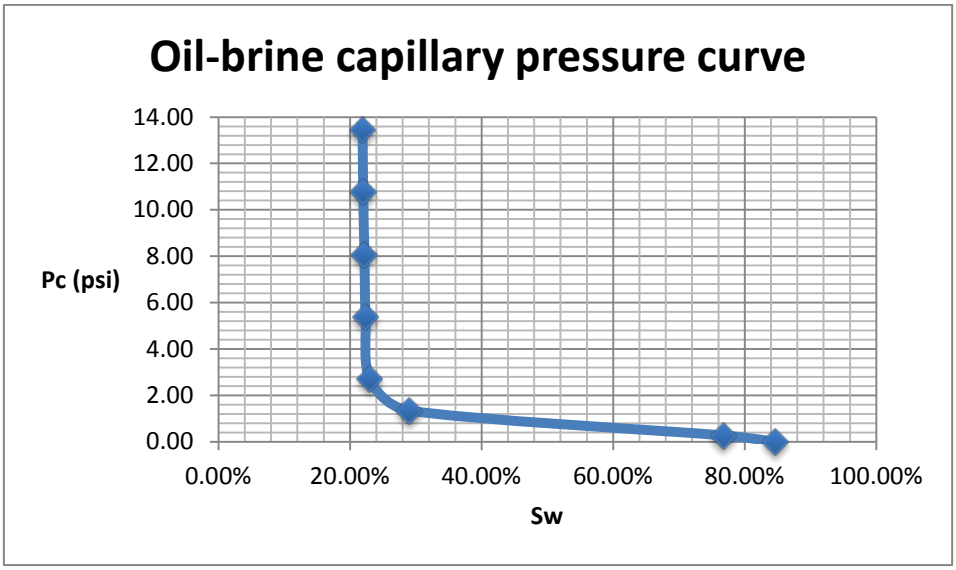

Figure 14. Oil-brine capillary pressure curve for Lagia-8 well (sample 1).

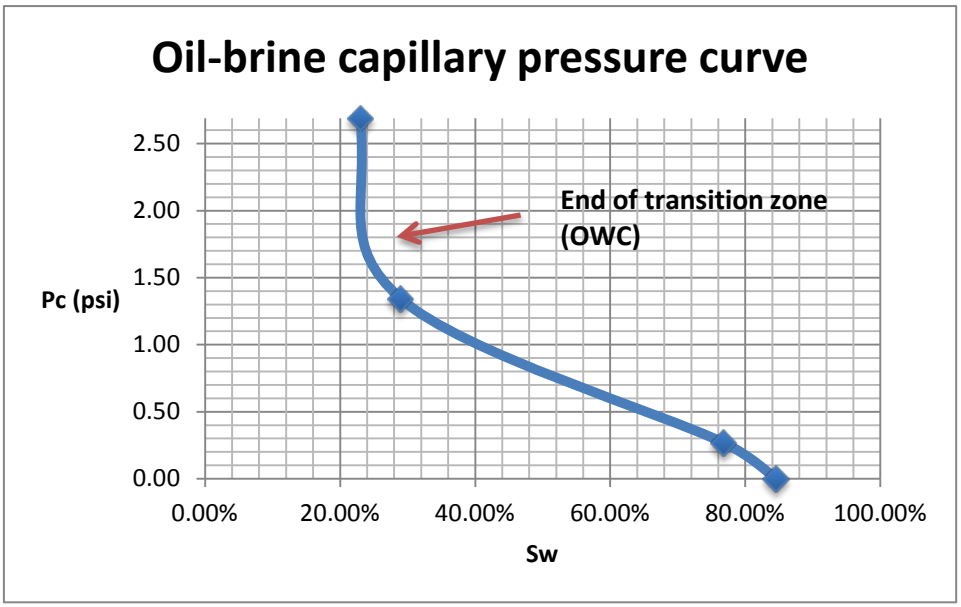

Figure 15. Oil-brine capillary pressure curve for Lagia-8 well (sample 2).

The disadvantages of the porous plate method are that it is time consuming. Also, capillary contact with the porous plate may be lost at high pressures. This causes erroneously high connate water saturations to be implied. Imbibition measurements are not generally attempted. While the advantage of the method is that the test plug has at least one representative fluid in place, i.e. the brine. This ensures that brine mineral interactions e.g. clay swelling, which affects pore size and surface states, are taken account of. This is a large advantage over the mercury method, which cannot take account of clay-water interactions.

II.4. Water Saturation Measurement

In order to measure values of original rock saturations there are two essentially methods: (1) The Retort method and (2) The Dean Stark method.

II.4.1. Retort method

The retort method apparatus is shown in Fig. (16), where the core is heated inside the sample cup causing the fluids to vaporize; oil and water are then condensed in the condensing tube and their volumes measured in the receiving tube.

The advantages to this method is the time for the experiment is short, typically less than 24 hours, and multiple samples can be run simultaneously. The disadvantages are heating process which burns oil to the pore surfaces. This is known as the cooking effect and thus results in oil recovery less than the initial amount in the sample.

The measured porosity is 28% from lab experiments with a bulk volume of 15.53 cm^3. After placing the sample in the retort, the receiving tube had 3.7 cm^3 of water and 0.9 cm^3 of oil. After correction, these readings according to calibration curves are:
V_{oil} = 1.1 cm^3, Soil = 25.3%, therefore S_g =7.9%, V_{water} = 2.9 cm^3 and S_{water} = 66.8%.

II.4.2. Dean Stark method

The Dean-Stark extraction method uses the vapor of a solvent to rise through the core and leach out the oil and water. The water condenses and is collected in a graduated cylinder. The solvent and oil continuously cycle through the extraction process. A typical solvent is toluene, miscible with the oil but not the water. Fig. (17) is an illustration of the apparatus (Robert P., 1980).

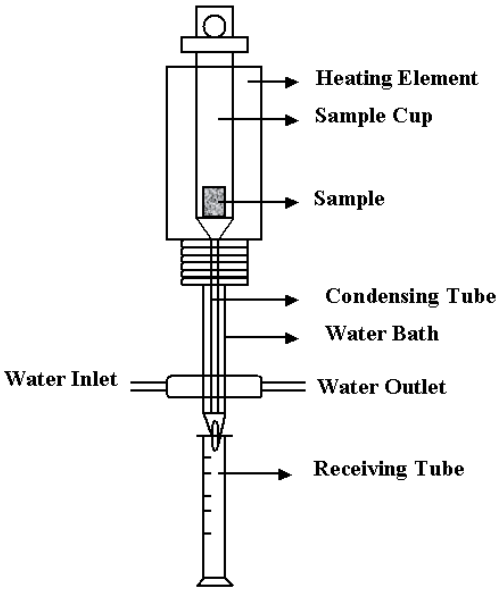

Figure 16. Retort apparatus.

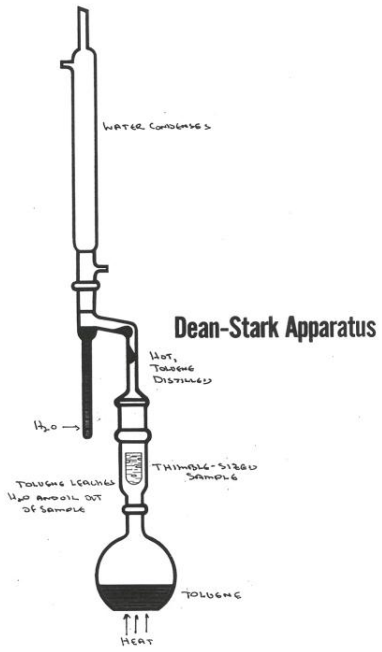

Figure 17. Dean Stark apparatus.

The volume of the collected water relative to the pore volume provides an estimate of the water saturation. The oil saturation is determined by:

$$S_o = \frac{W_{initial} - W_{dry} - \rho_w V_w}{\rho_o V_p} \quad (29)$$

That is, by the weight loss not accounted for the water, equation (29) requires the weight of the core prior to the test (W_i), the weight of the core after the test cleaned and dried (W_{dry}), the pore volume from other methods (V_p) and an estimation of the oil density (ρ_o).
The following items are the results:

V_{bulk} of sample = 30.1 cm^3, V_{water} = 5.6 cm^3, Porosity = 29.1%, Saturation of water = 61.6%, Oil specific Gravity = 0.83, W_{intial} = 67.2 grams, W_{dry}= 59.6 grams, Water mass = 5.6 grams, V_{oil} = 2.4 cm^3 and S_{oil} = 27.2 %.

III. WELL LOGGING INTERPRETATION OF LAGIA-8

The present study deals with the petrophysical evaluation of Nukhul Formation at Lagia-8 well in Sinai. This study was done utilizing different types of open-hole well log; for the determination of the petrophysical parameters. These logs are: gamma-ray, neutron, density and resistivity. The analytical well logging system is started by recalibrating and correcting the logging data of the chosen boreholes (Gunter, et al 1997). In oil field logging applications, the prime importance is directed to define the types and amounts of fluids encountered in the formations (Asquith, 2004 and Bassiouni, 1994). These determinations require the calculation of the formation porosity, consequently the estimation of the shale volume. In other words, shale volume is needed for correcting the porosity and water saturation results for the biased effects of shale (Horne, 1995 and Helander, 1983).

III.1. Average Porosity

The average porosity was determined at depth 1296 ft. by using the data from the density and neutron logs, according to the Wyllie, equation (1963).

$$\rho_b = \rho_{ma} * (1 - \emptyset) + \rho_f * \emptyset \qquad (30)$$

From density logs ρ_b = 2.45 gm/cm^3, and the density of fluid = 1 gm/cm^3 (approximately density of formation fluids). The value of the matrix density represents sandstone formation, so ρ_{ma}= 2.65 gm/cm^3. The calculated porosity from density and neutron logs is about 0.20.

By using the density-neutron crossplot (Sclumberger, 2009) as shown in Fig. (18), it is found that the porosity is to be 0.121 in a sandstone formation with a percentage of calcite.

While at depth 1297 ft., the average porosity is 0.105 through using of the following parameters: density of matrix = 2.65 gm/cm^3 (default density of quartz sandstone), density of fluid = 1 gm/cm^3 and bulk density = 2.477 gm/cm^3 (from log).

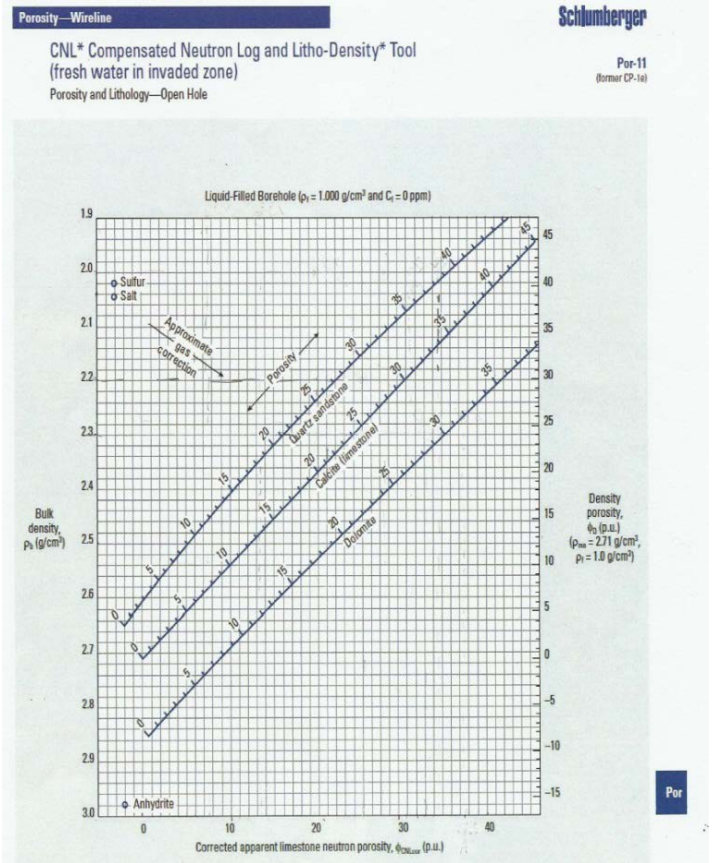

Figure 18. Porosity-lithology relationship.

III.2. Wyllie-Rose Permeability

The permeability of a rock is a measure of the ease with which the rock will permit the passage of fluids. Permeability from the Wyllie-rose method, (1950) is one of the oldest permeability methods available, and is reliable when calibrated to core data.

Wyllie-Rose of Gulf Oil fame (Fig. 19), was the first researchers to publish a relationship between permeability, effective porosity and irreducible water saturation as follow:

$$k = \frac{C\,\varphi_{eff}^{6}}{S_{wirr}^{2}} \qquad (31)$$

The constant C = 62,500 in oil and C = 6241 in gas. Morris and Biggs of Schlumberger, (1967) tweaked this relationship with constant C = 65,000 for oil and C = 6,500 for gas. Turk Timur of Chevron (1968) performed more empirical studies and published an improved correlation:

$$k = \frac{C\,\varphi_{eff}^{4.4}}{S_{wirr}^{2}} \qquad (32)$$

where the constant C = 3,400 for oil and C = 340 for gas .

So when using this modules, there are a choices for using the empirical correlations. The most difficult part is computing the irreducible water saturation in the zones that permeability is computed by using this module. Also effective porosity must be computed by some methods.

The effective porosity is calculated by the following equation:

$\Phi_{E1} = \Phi_T \times (1 - V_{sh})$ (33)

The irreducible water saturation can be estimated by Crain's method (1986), from the general formula:

$S_{wirr} = \Phi \times S_w / \Phi_{eff}$ (34)

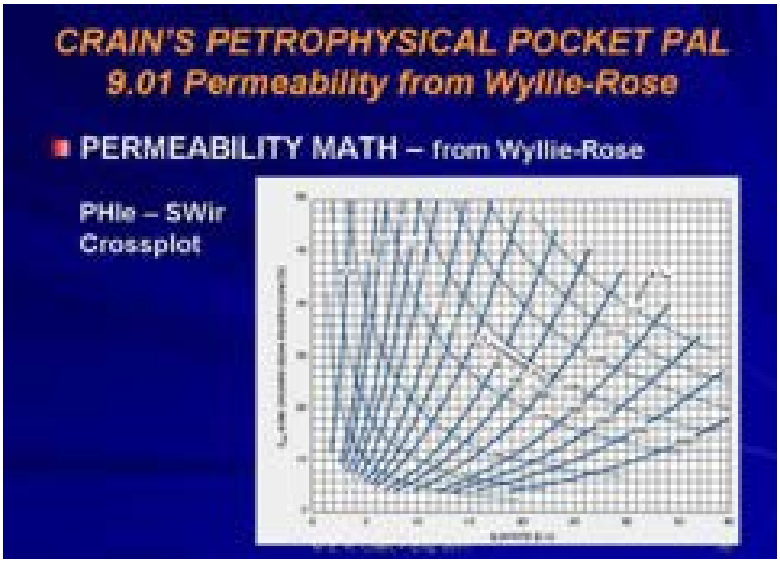

Figure 19. Wyllie-Rose permeability

The calculated permeability from this method is 60.245 mD. at depth 1296 ft. and it is about 203.79 mD. at depth 1297 ft., the results are shown in Figs. (20 and 21).

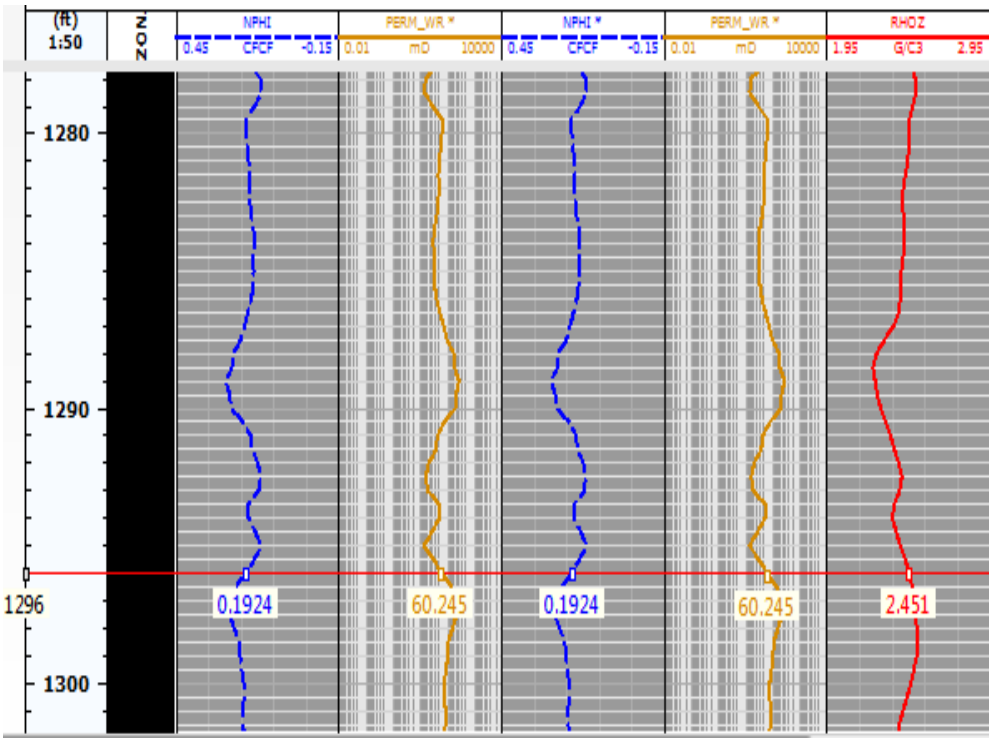

Figure 20. Permeability log at 1296 ft.

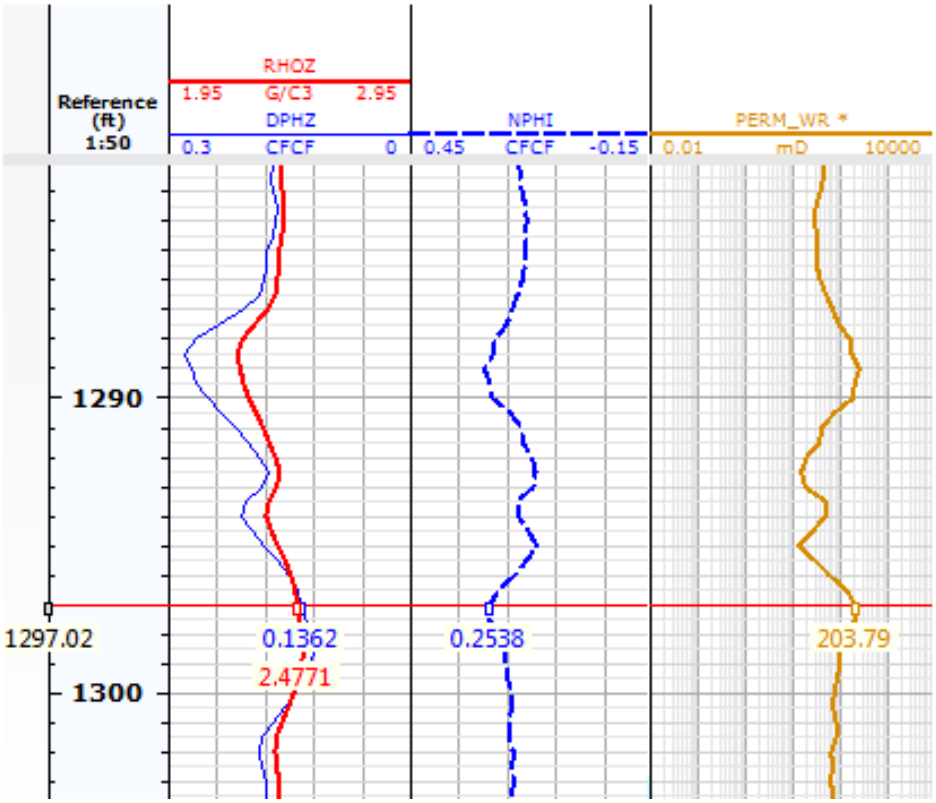

Figure 21. Permeability log at 1297 ft.

III.3. Water Saturation

To calculate S_w from Archie's equation (1942) based on the reading of the well logs we had to first determine the empirical constants of Archie's equation for the best suites to our case study. A sample of the formation water was extracted and processed in the lab and the R_W of the water was measured at a room temperature which was 0.07 Ω.m., Rw is corrected according to the down-hole temperature by using the geothermal gradient of 1 ^oF / 70 feet. Therefore, the calculated temperature at the depth of the pay zone is

Z.T = Temperature Surface + (depth * Geothermal. gradient) (35)

Accordingly, the zone temperature is 94 ^oF, and the corrected value of R_w is 0.054 Ω.m.

Based on several core samples of different fluid saturations, the empirical constants R_w, m, n and a were calculated at given values of porosity and saturation (Tiab, 1997).

$$n\log(S_w) = \log(a.R_w) - m.\log(\varphi) - \log(R_t) \quad (36)$$

Using 4 different saturations from the capillary pressure experiment we can solve for the 3 unknowns. To obtain four different saturations the core plugs are cleaned in the dean stark and then saturated completely with formation water and then placed in the capillary pressure device where pressurized air force the water out of the sample. Different pressures applied each time to obtain different saturations. S_w is calculated each time by measuring the difference in weight which is explained thoroughly in the capillary pressure sections shown in Table (14). Each time after saturating core sample R_t is measured.

Table 14. Water saturation, true resistivity and porosity readings.

S_w	R_t / Ω.m	φ
84.59%	1.2502	0.2795
76.76%	1.5170	0.2795
28.97%	10.6136	0.2795
23.01%	16.8083	0.2795

The estimated empirical constants are as follow: n= 1.996, m= 1.999, a=1.0003 and R_w = 0.07 Ω.m. Thus no temperature correction is needed. By using the value of the deep resistivity which is 4.60 at depth 1297 ft., the value of water saturation is 48.5%.

III.4. Capillary Pressure

Aguilera, (2001) published an empirical relationship incorporating the capillary pressure, as follow:

$Pc = (Swi^{-0.8} * \Phi^{-2.25}) /0.929$ (37)

where: porosity and water saturation are expressed as fractions which is calculated from the previous equation.

IV. DATA CORRELATION AND ANALYSIS

IV.1. Average Porosity

Measurement of porosity by using core analyses is very accurate and is a rapid technique. The value of the average porosity is about 28%, while that measured from well logging gives a range value about 21%. This is the closest value estimated by using density and neutron tools.

IV.2. Permeability Results

According to the given results, measurements of absolute permeability using liquid permeability and Wyllie-Rose correlation are closer to each other, which mean that they are more reliable. Gas permeability however gave very small result compared to the other methods. This could be due to many reasons, including the fact that the experiment was conducted using nitrogen gas instead of air as Klinkenberg correction (1941), who assumes that the core sample is saturated with air. Another reason could be that the outlet pressure P_2 was set to atmospheric pressure, which results in error in readings of flow rate.

The permeability using Wyllie-Rose correlation is derived from density porosity, which means that it might not be always close to the true value of permeability as porosity and permeability do not follow a definite pattern. This leaves us with the permeability value measured using the liquid permeability (William, 1990). Theoretically, this result is supposed to be the most reliable. However, the core might be damaged during transportation from the field to the lab, which reduces effective porosity; ultimately reducing permeability. The permeability results for Lagia – 8 well, are shown in Table (15).

Table 15. Permeability results for Lagia -8 well.

$K_{abs.}$ from gas permeability		$K_{abs.}$ from liquid permeability	$K_{abs.}$ from Wyllie-Rose correlation	
Sample 1: 2.80 mD.	Sample 2: 5.53 mD.	Sample 1: 166.82 mD.	@1296 ft.: 203.79 mD.	@1297 ft.: 60.245 mD.

IV.3. Capillary Pressure Results

By comparing the capillary pressure curve obtained from the lab experiment with the capillary pressure curve constructed using the well logs, we can readily observe the conformity of the values of both curves since the values of capillary pressure from both curves at the same water saturation are very close to each other. This proves the validity of the experimental data achieved using the porous plate experimentand enhances the reliability of the study. Based on the magnified capillary pressure curve, we can determine the end of the transition zone, or in other words, the oil-water contact, which lies at a capillary pressure of 7 psi.

To further ensure the accuracy of the lab experiment, we can calculate the thickness of the transition zone using equation (38), and see how close it is to the thickness value obtained from the well logs (18 ft).

$$\text{Transition zone thickness} = \frac{144P_c}{\rho_w - \rho_o} = \frac{144 \times 1.8816}{67.416 - 51.81} = 17.36 \text{ ft} \quad (38)$$

Since, this calculated value of transition zone thickness is very close to the value of thickness of 18 ft, which is obtained from the logs; therefore, the experimental data are accurate and representative of the studied reservoir.

IV.4. Water Saturation

The estimated water saturation from the two methods of core analyses is near to each other, the first reading is 66.8% from Retort method while another value is 61% from Dean Stark method. But in case of well logging analysis, the value of estimated water saturation is 48.5% which is far from the values of the core analysis. Then the results from cores are very

accurate and take a short time and do not need the calculation of temperature or any corrections.

CONCLUSION

Core analysis generally gives more accurate indications of well parameters as it involves real measurements of actual samples from the reservoir rock, however, several reservoir parameters are not into consideration in core analysis such as reservoir temperature and pressure, reservoir heterogeneity, invasion effects, and gas effects, etc. Core analysis is beneficial in calculating the empirical constants of Archie's equation using regression analysis, but it is not efficient in detecting faults because the core plug is only a small sample of the reservoir rock. For better core analysis, larger core samples are needed but it is not always efficient because core analysis devices function on the small core samples only. Determining porosity using core analysis has the advantage that it excludes assumptions on mineral composition, borehole effects, etc. However, porosity values obtained from core analysis are frequently more accurate in heterogeneous reservoirs.

Relative permeability gives an indication of the ability of a single phase fluid to flow in presence of multiphase fluids. Knowing relative permeability allows us to estimate recoveries at certain water saturations. However, measuring relative permeability for a core sample is not an indication for the entire well. Therefore, correlations of overall curve shape, cross-over points, formation water permeability at residual oil saturation etc., must all be made with reference to lithology, permeability, and initial fluid saturations. Relative permeability measurements are affected by fluid saturation, saturation history, and magnitude of initial-phase saturations, wettability, rock pore structure effect, overburden stress, clay and fines content, temperature, interfacial tension and viscosity, and displacement rates. Parameters such as overburden stress, clay and fines content and migration, reservoir temperature, and saturation history may not be taken into consideration through core analysis, but since no logs give relative permeability values, it is essential to conduct relative permeability experiments in the lab.

By comparing the capillary pressure curve obtained from the lab experiment with the capillary pressure curve constructed using the well logs; we can readily observe the conformity of the values of both curves where the values of capillary pressure from both curves at the same water saturation are very close to each other. This proves the validity of the experimental data achieved using the porous plate experimentand enhances the reliability of the study.

Based on the above magnified capillary pressure curve, we can determine the end of the transition zone, or in other words, the oil-water contact, which lies at a capillary pressure of 7 psi. Also from the previous results, Nukhul Formation in Lagia-8 well can be accepted as a good reservoir rock.

REFERENCES

Aguilera, R., (2001): Incorporating capillary pressure, pore throat aperture radii, height above free-water table, and Winland r35 values on Pickett plots: AAPG Bulletin, v.86, no.4, p. 605-620.

Ahmed, T (2006): Reservoir engineering handbook. 3rd Edition. Elsevier Inc. Print.

Amyx, J.W., Bass, D.M., and Whiting R.L. (1960): Petroleum reservoir engineering, McGraw- Hill, New York, NY

Archie, G.E. (1942): The Electrical resistivity log as an aid in determining some reservoir Ccharacteristics. Trans., AIME, v. 146.

Asquith, George and Daniel Krygowski (2004): Basic well log analysis. The American Association of Petroleum Geologists. Print.

Bassiouni, Zaki (1994): Theory, measurement, and interpretation of well logs. SPE. Print

Bed, Buwy A. Jr. and Nunes, Craig S. (1984): Velocity and gravity effects in relative permeability measurements. Stanford University Press.

Charles M. Marle (1981): Multiphase flow in porous media, editions Technip, Paris

Crain, E.R. (1986): The log analysis hand book; Penn-Well, Publ. Co., Tulsa, Oklahoma, U.S.A.

Dandekar, Abhijit Y. (2006): Petroleum reservoir rock and fluid properties. Boca Raton, FL: CRC/Taylor & Francis.

Engler, T.W. (2003): Fluid flow in porous media – Notes of Class Petroleum Engineering 524 – Fall 2003.

Glover, Paul (2001): Formation evaluation. University of Aberdeen Press, United Kingdom.

Glover, Paul (2012): Petrophysics. Abardeen: Department of Geology and Petroleum Geology University of Aberdeen UK.Web. 1 May 2013.

Gunter, G.W. J. J. Pinch, J. M. Finneran, and W. T. Bryant (1997): Overview of an integrated process model to develop petrophysical based reservoir descriptions: Society of petroleum Engineers Annual Technical Conference, SPE paper 38748, p. 5.

Helander, D.P. (1983): Fundamentals of formation evaluation, OGCI Publications, Tulsa, OK.

Holditch, S. A. and R. A. Morse (1998): The effects of Non-Darcy Flow on the Behavior of Hydraulically Fractured Gas Wells. Journal of Petroleum Technology. SPE.Web. 29 April 2013.

Horne, R. (1995): Modern well test analysis. Petroway, Inc., p. 257.

Klinkenberg, L. J. (1941): The permeability of porous media to liquids and gases, Drilling and Production Practice, American Petroleum Inst., p. 200–213

Morris, R.L. and Biggs, W.P. (1967): Using log-derived values of porosity and water saturation, Trans. SPWLA, 7th Annual Logging Symposium, Denver, June 11-14, Paper X.

Robert P. Monicard (1980): Properties of reservoir rocks: Core analysis, Editions Technip, Paris

Sandberg, C. R., Gournay, L. S., and Sippel, R. F (1993): The effect of fluid flow rate and viscosity on laboratory determinations of oil-water relative permeability. Petroleum Transactions, AIME, v. 213.

Schlumberger Manual (2009): Basics of well logging interpretation, Introduction to Open-hole Log Interpretation.

Tiab, Djebbar, and Erle C. Donaldson (1997): Theory and practice of measuring reservoir rock and fluid transport properties. Houston, Tex: Gulf Pub. Print.

Timur, Turk (1968): An investigation of permeability, porosity and residual water saturation relationships," Ninth Annual Logging Symposium, SPWLA Transactions, June 23-26, paper J.

William D. McCain. (1990): The properties of Petroleum fluids – Second edition, Pennwalt books, Oklahoma.

Wyllie, M.R.J. and Rose, W.D. (1950): Some theoretical considerations related to the quantitative evaluation of the physical characterization of reservoir rock from electric log data," *Trans*. AIME, Vol 189, p. 105.

Wyllie, M.R.J. (1963): The fundamentals of well log interpretation; New York Academic Press.